environments

MDPI

Article

Microbial Contamination and Sterilization Methods in an Air Circulation-Type Geothermal Ventilation System

Hyuntae Kim

Kurume Institute of Technology, Kamitsu-machi, Kurume 2228-66, Japan; kim@kurume-it.ac.jp

Abstract: A simulated system was created to evaluate an air circulation-type geothermal ventilation system, focusing on measuring microbial contamination levels on the surface of the heat exchange unit. Additionally, this study examined sterilization methods using UV lamps on the surface of the heat exchanger. The fungal concentration on the surface of the heat exchanger showed a tendency to increase over time. Although direct comparison is challenging due to the varying concentrations of outdoor air fungi at different measurement times, the surface fungal concentration was highest at a minimum airflow rate of 150 m^3/h compared to other conditions. However, since the adhesion of contaminants from outdoor air to the surface of the heat exchanger is influenced not only by airflow but also by outdoor temperature and relative humidity conditions, future research needs to consider these factors. According to the ATP measurement results, microbial contamination was evaluated as "slightly dirty" after 24 h and "dirty" after 48 h of operating the experimental apparatus. Therefore, it is advisable to clean the internal surfaces of the geothermal ventilation system every 1–2 days. The results of the sterilization experiments using UV lamps indicated that irradiation for approximately 30 min inactivated 94.5%-to-96.1% of microorganisms derived from outdoor air. However, since the sterilization dose varies depending on the type of microorganism, it is necessary to determine the optimal irradiation time based on the target microorganisms and the UV lamp's irradiation intensity.

Keywords: geothermal ventilation; fungal; UV lamps

Citation: Kim, H. Microbial Contamination and Sterilization Methods in an Air Circulation-Type Geothermal Ventilation System. *Environments* **2024**, *11*, 254. https://doi.org/10.3390/environments11110254

Academic Editor: William A. Anderson

Received: 4 September 2024
Revised: 12 November 2024
Accepted: 13 November 2024
Published: 14 November 2024

1. Introduction

The Japanese government has set a goal of achieving zero greenhouse gas emissions by 2050 as part of its measures to combat global warming and has expressed its commitment to this goal [1]. As of the 2016 fiscal year, the civilian sector accounted for approximately one-third of Japan's carbon dioxide emissions [2]. Consequently, there is a need to reduce energy consumption in buildings such as residences, hospitals, schools, and office buildings. The utilization of renewable energy is effective in reducing carbon dioxide emissions in the civilian sector, leading to increased use of natural energy sources such as solar power, solar heat, wind power, and geothermal energy. However, natural energy sources are highly dependent on weather conditions, making it difficult to ensure a stable energy supply. In contrast, geothermal energy systems can provide relatively stable energy compared to other natural energy sources, making them highly valuable. Geothermal energy utilization includes systems such as geothermal heat pumps and air circulation-type geothermal systems [3]. The method of utilizing geothermal energy should be selected based on the type and purpose of the building. According to Hasegawa et al., ground temperature is influenced by the soil's thermal conductivity, heat capacity, and regional outdoor temperature variations, and the depth at which the annual average outdoor temperature is maintained is approximately 5–6 m [4]. However, when installing a cool tube at this depth in actual residential settings, there are difficulties due to the cost of excavation and potential reduction in ground bearing capacity. Therefore, Tarumizu et al. examined the effectiveness of geothermal energy utilization in residences by burying heat and cool tubes at a depth of approximately 2 m and calculating the heat removal in summer and

heat acquisition in winter [5]. Previous studies on cool tubes include investigations of cooling effects and factors affecting performance in experimental houses and numerical analyses of the thermal performance of natural ventilation-driven cool tube systems [6–13]. The authors have been conducting research on the thermal performance evaluation of geothermal ventilation systems and the removal of outdoor-derived contaminants [14,15].

However, since the air circulation-type geothermal ventilation system directly introduces outdoor air into the pipes, airborne fungi, dust, pollen, and PM2.5 from outdoor air are likely to be conveyed into the system, contaminating the surfaces of the heat exchange pipes with outdoor-derived pollutants. Particularly, condensation on the surfaces of geothermal pipes may significantly promote microbial growth.

In this study, a simulation system representing an air-circulating geothermal ventilation system was created, and two experiments were conducted. The first experiment measured the level of microbial contamination on the surface of the heat exchange unit. After confirming microbial contamination on this surface, the second experiment investigated a sterilization method for the inner surface of the system's piping.

2. Materials and Methods

Figure 1 shows the floor plan and the A–A′ cross-sectional view of the laboratory. The experimental apparatus was installed in an environmental laboratory with adjustable temperature settings. The laboratory dimensions are 7.3 × 7 m, with a ceiling height of 2.5 m. The entrance of the simulated geothermal heat exchange unit is open to the outside of a window, allowing outdoor air to be drawn into the apparatus. A ventilation fan was installed at the indoor end of the simulated unit to draw in outdoor air. Figure 2 provides a detailed cross-sectional view of the simulated geothermal heat exchange unit. The simulated unit was designed to mimic the geothermal heat exchange part of an air circulation-type geothermal ventilation system [14]. The length of the simulated unit is 2.6 m, with a duct cross-section of 280 × 300 mm. The simulated unit utilized 30 mm-thick insulation material. The inner surface of the simulated unit was finished with aluminum tape. An aluminum flat plate, identical in material to the heat exchange part of the air circulation-type geothermal ventilation system, was installed on the bottom surface inside the simulated unit. The aluminum plate dimensions are 3 × 250 × 2000 mm. To replicate the surface temperature of the geothermal heat exchange part, a silicone tube was placed under the aluminum plate, and cold water was circulated to cool the aluminum plate. The cold water was generated using a cooling water circulation unit (LTC-1200α).

This laboratory is generally not open to the public, and its air is directly exhausted to the outside. Additionally, measurements were taken while wearing sanitary gloves and laboratory attire to prevent contamination from human-derived microorganisms. Figure 3 shows photographs of the experimental apparatus.

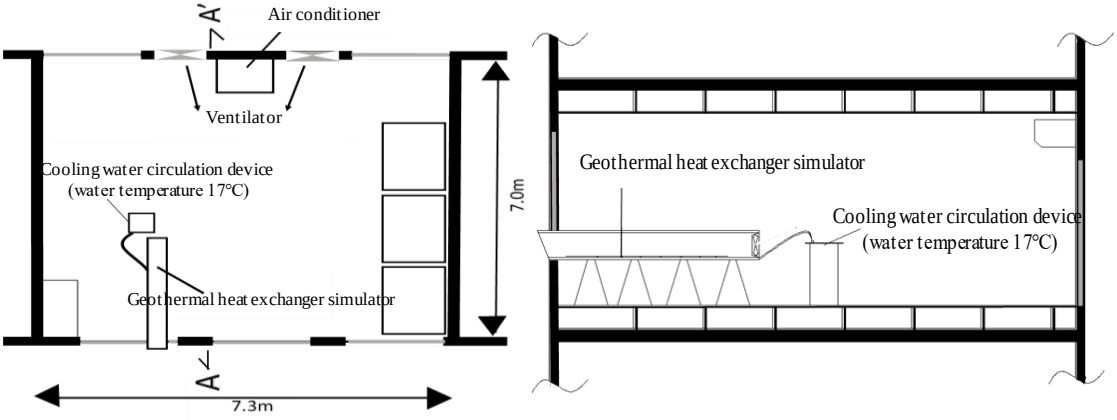

Figure 1. The floor plan and the A–A′ cross-sectional view of the laboratory.

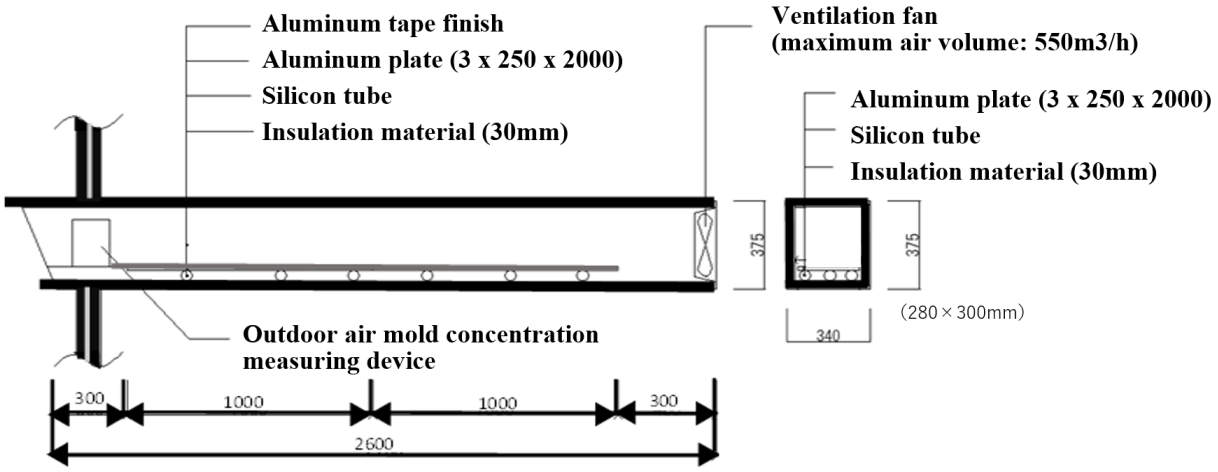

Figure 2. The detailed cross-sectional view of the simulated geothermal heat exchange unit.

Figure 3. The photographs of the experimental apparatus.

3. Measurement Overview

3.1. Measurement Conditions

The soil temperature around the air circulation-type geothermal pipes measured in our laboratory was between 17 and 20 °C [14]. Therefore, the temperature of the cold water supplied by the cooling water circulation unit was set to 20 °C. The air circulation-type geothermal ventilation systems are often installed in residences, educational facilities, gymnasiums, etc. Based on the airflow rates of actually implemented systems, the airflow rates through the simulated apparatus were set to 150 m^3/h, 300 m^3/h, and 550 m^3/h.

3.2. Measurement Methods

Table 1 details the measurement instruments. To understand the contamination status on the surface of the aluminum plate, the fungal concentration on the surface of the aluminum plate installed inside the simulated apparatus was measured using stamp-type agar media. Additionally, the ATP (Adenosine triphosphate) amount, which indicates the level of microbial contamination, was measured. The airborne fungal concentration in the outdoor air was also measured using a mold sampler. Before measurement, the surface of the aluminum plate was washed with water and sterilized with alcohol. Figure 4 shows the measurement instruments and the measurement process.

Table 1. The details of the measurement instruments.

Measurement Item	Measuring Device Model Number
Fungal concentration in outdoor air	Mold Sampler (IDC-500B)
Surface ATP concentration	Highly sensitive luminometer (EnSURE) ATP swab test reagent (Supersnap)
Surface fungal concentration	Stamp-type agar medium (PDA)

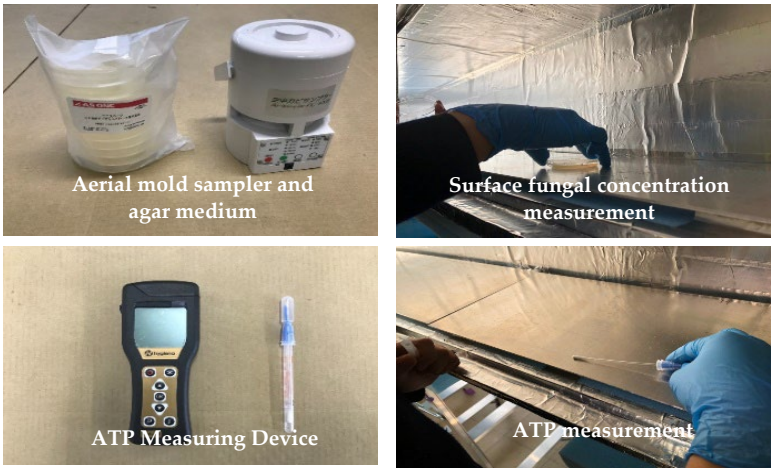

Figure 4. The measurement instruments and the measurement process.

(1) Airborne Fungal Concentration

The airborne fungal measurement referred to the environmental standards of the Architectural Institute of Japan [16]. For measuring the fungal concentration in the outdoor air, a mold sampler (IDC-500B) was installed at the outdoor air intake part of the simulated apparatus, and outdoor air was collected. Potato Dextrose Agar (PDA) for fungi was used. The suction volume of the outdoor air was 100 L. The incubation conditions were at a temperature of 25 °C for 3–5 days, and the colony count was recorded. The colony count unit was cfu/m^3. Fungal concentrations in the outdoor air were measured outside the laboratory in mid-September 2022, during a hot and humid period.

(2) Surface ATP Amount

ATP measurement utilizes the reaction between ATP, which is present in all living organisms, and a reagent that emits light, with the relative light emission being measured [17]. ATP was measured using a high-sensitivity luminometer (EnSURE) and the Supersnap ATP swab test reagent. Table 2 shows the contamination levels for ATP measurements in terms of cleanliness evaluation [18]. The cleanliness evaluation referred to previous studies, and the measurement results were evaluated per 100 cm^2 [19,20].

Table 2. The contamination levels for ATP measurements in terms of cleanliness evaluation [18].

Level	Evaluation Criteria	
I	Extremely clean	0~100
II	Very clean	110~300
III	Usually clean	310~800
IV	A little dirty	810~2000
V	Dirty	2010~5000
VI	Very dirty	5010~10,000
VII	Extremely dirty	10,010~

(3) Surface Fungal Concentration

The fungal concentration on the aluminum plate surface was measured using stamp-type PDA. The incubation temperature was 25 °C for 3–5 days, and the colony count was recorded.

3.3. Measurement Points and Schedule

Figure 5 details the measurement points on the aluminum plate. Figure 6 shows actual photos of the aluminum plate. As the width of the aluminum plate is 25 cm, leaving 2.5 cm on each end, the measurement area was divided into 20 cm (width) × 200 cm (length), containing 160 squares of 5 × 5 cm each (40 locations horizontally, 4 locations vertically). As shown in Figure 5, the aluminum plate was divided into three sections along its length: I, II, and III. For each measurement, two sampling points (a, b) were taken in sections I, II, and III for the surface fungal concentration measurement.

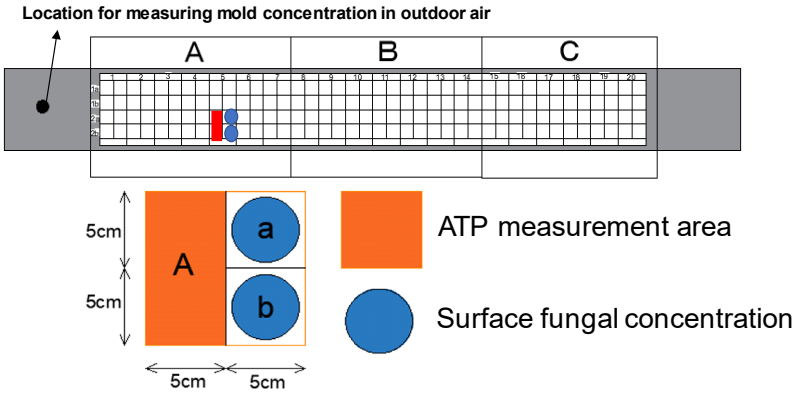

Figure 5. The measurement points on the aluminum plate.

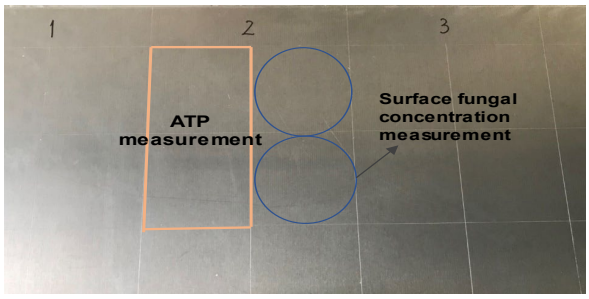

Figure 6. The actual photos of the aluminum plate.

For ATP concentration, two squares were treated as one unit, and the measurement surface (A) was evaluated. The reason for increasing the ATP measurement area was to avoid missing data. For each ATP measurement, one sampling point was taken in sections I, II, and III. Table 3 shows the measurement schedule. The surface fungal concentration and surface ATP amount were measured on the sterilized surface of the aluminum plate on days 0, 1, 2, 3, 5, and 7. On day 0, measurements were taken every 3 h starting at 9 AM, with a total of four measurements: twice in the morning (9 AM, 12 PM) and twice in the afternoon (3 PM, 6 PM). On days 1, 2, 3, 5, and 7, measurements were taken once in the morning (9 AM). The airborne fungal concentration was measured four times on day 0, every 3 h from the start of the measurement, and once in the morning (9 AM) on days 1, 3, 5, and 7.

Table 3. The measurement schedule.

Schedule	Time	Surface ATP Concentration	Surface Fungal Concentration	Fungal Concentration in Outdoor Air
Day 0	0 h	Measure one place each in areas I, II, and III	Measure two places each in areas I, II, and III	The fungal concentration in the outside air was measured twice
	3 h			
	6 h			
	9 h			
Day 1	24 h			
Day 2	48 h			
Day 3	72 h			
Day 5	72 h			
Day 7	168 h			

3.4. Results and Discussion

3.4.1. Fungal Concentration in Outdoor Air

Figure 7 shows the fungal concentration in outdoor air under various conditions. The fungal count result is the total microorganisms that grew on the medium. The fungal units are expressed in cfu/m^3. For the condition with an airflow rate of 150 m^3/h, the average fungal count in outdoor air was 349 cfu/m^3, with a minimum and maximum of 125 and 895 cfu/m^3, respectively. At an airflow rate of 300 m^3/h, the average fungal count was 362 cfu/m^3, with a minimum and maximum of 160 and 1025 cfu/m^3, respectively. For an airflow rate of 550 m^3/h, the average fungal count in outdoor air was 449 cfu/m^3, with a minimum and maximum of 170 and 790 cfu/m^3, respectively. Comparing the average fungal concentrations in outdoor air across the measurement periods for each airflow rate, the condition with an airflow rate of 550 m^3/h showed the highest concentration.

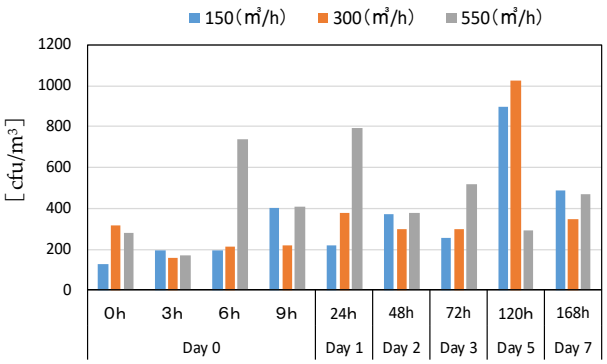

Figure 7. The fungal concentration in outdoor air under various conditions.

3.4.2. Surface Fungal Concentration

Figure 8 shows the temporal change in fungal concentration on the surface of aluminum plates. The fungal counts are converted to values per unit area. The fungal concentration on the aluminum plate surface increased over time. After 168 h, the surface fungal concentration was approximately 74,000 cfu/m^2 under the 150 m^3/h airflow condition and approximately 49,000 cfu/m^2 under the 300 m^3/h airflow condition. The 550 m^3/h airflow condition reached its peak at 120 h, with approximately 65,000 cfu/m^2. In all conditions, the surface fungal concentration within the device increased over time. It was challenging to determine the extent of the impact of airflow on surface fungal concentration. The authors hypothesized that slower airflow conditions would result in higher fungal counts and that faster airflow conditions would reduce the number of fungi adsorbed on surfaces.

However, the fungal count under the 550 m^3/h condition was higher than that under the 300 m^3/h condition, contrary to the authors' hypothesis. This discrepancy is attributed to differences in factors such as the concentration of fungi in the outdoor air introduced into the device, temperature, relative humidity, and surface condensation conditions.

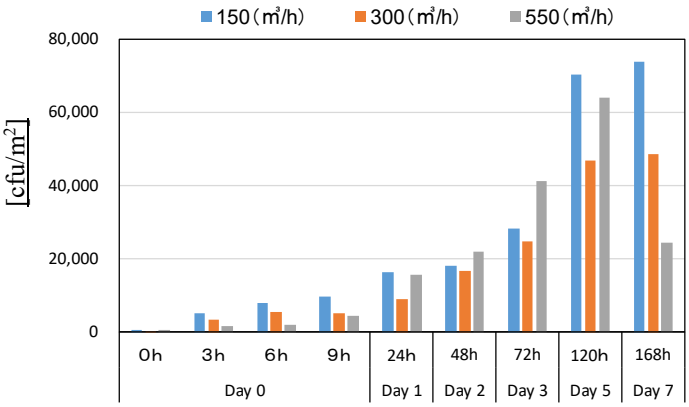

Figure 8. The temporal change in fungal concentration on the surface of aluminum plates.

3.4.3. Surface ATP Levels

Figure 9 shows the temporal change in ATP measurements on the surface of aluminum plates. ATP values are for all microorganisms from outside air. The unit for ATP is the RLU (Relative Light Unit). Table 2 was used for the assessment of contamination levels. The ATP measurements immediately after washing the aluminum plate surfaces with water and disinfecting with alcohol ranged from 6 to 11 RLU for all conditions, with the contamination level rated as "very clean." Over time, the surfaces of the aluminum plates gradually became contaminated. At airflow rates of 150 m^3/h and 300 m^3/h, the ATP measurements exceeded 810 RLU after 24 h, with a contamination level rated as "slightly dirty". For the 550 m^3/h airflow condition, the ATP measurements exceeded 2010 RLU after 48 h, with a contamination level rated as "dirty". Figure 10 shows the correlation between surface fungal counts (cfu/25 cm^2) and ATP measurements (RLU/25 cm^2). The surface fungal counts and ATP measurements are converted to values per area of one agar plate (25 cm^2). The correlation coefficient was R^2 = 0.6843, indicating a certain correlation between fungal counts and ATP measurements. While measuring fungal counts using agar plates is time-consuming and labor-intensive, if fungal counts can be predicted by ATP measurements, ATP measurements could serve as an effective and simple method for field assessments.

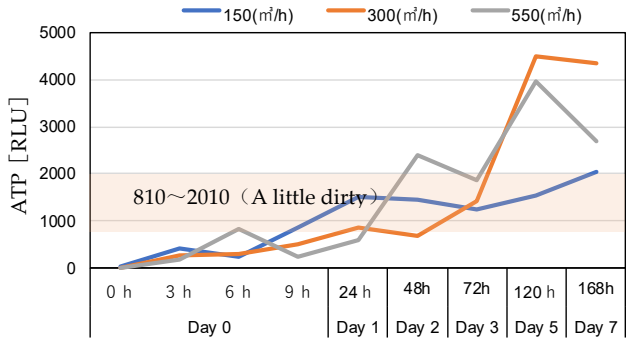

Figure 9. The temporal change in ATP measurements on the surface of aluminum plates.

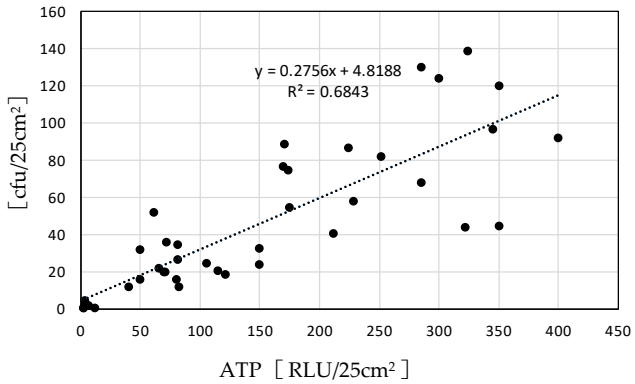

Figure 10. The correlation between surface fungal counts (cfu/25 cm^2) and ATP measurements (RLU/25 cm^2).

4. Sterilization Effect of UV Lamps

Using a simulated experimental apparatus, the microbial contamination on the surface of the geothermal heat exchange unit was measured, confirming that the surface is contaminated with microorganisms in a short period. According to Yanagi, microbial contamination within heating and cooling systems can lead to the generation of mold odors and deteriorate indoor air quality [21]. Furthermore, to create an environment where microorganisms cannot proliferate, proper maintenance, removal of contamination sources, and the use of technologies to inhibit microbial growth, such as ultraviolet (UV) sterilization and ozone sterilization, are necessary. Various measures can be taken to prevent microbial contamination in air conditioning systems. The authors measured the surface sterilization effect of UV lamps.

4.1. Confirmation of Ultraviolet Intensity

Many commercially available ultraviolet lamps emit 254 nm UVC, which is highly effective for disinfection, using low-pressure mercury lamps. The required ultraviolet (UV) dose for microbial disinfection varies depending on the type of microorganism. The UV dose [J/m^2] from a UV lamp can be calculated by multiplying the UV intensity [W/m^2] by the exposure time [s] [22]. Since the commercially available UV lamps did not display the UV intensity information, the UV intensity was measured using a UVC sensor (Lutron YK-37UVSD). Figure 11 shows the measurement positions and photos of the UV intensity measurement. The UV intensity was measured by placing the UV lamp inside the experimental setup and positioning the UVC sensors at three locations (①, ②, ③), as shown in Figure 11. The distance from the UV lamp to the UVC sensors was approximately 28-to-30 cm. The average UV intensity at the three locations was 0.156 mW/cm^2.

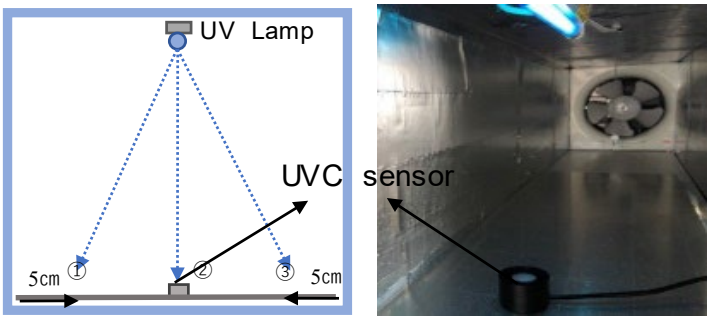

Figure 11. The measurement positions and photos of the UV intensity measurement.

4.2. Experimental Overview

The sterilization experiment using UV lamps was conducted within the simulated apparatus described in Chapter 2. The target microorganisms for sterilization were *As-*

pergillus niger (NBRC 6341) and *Penicillium pinophilum* (NBRC 6345), as these are the most common fungi found in the air. The sterilization exposure doses for these two species were 264 and 26.4 mW·s/cm^2, respectively, which are sufficient to achieve 99.9% sterilization on culture media [22]. For this experiment, the exposure time was determined based on the higher sterilization exposure dose required for *Aspergillus niger* (NBRC 6341). Table 4 shows the experimental conditions for sterilization (levels of exposure doses). The exposure time for each condition is the cumulative time. Before the sterilization experiment, the aluminum plates, which were the measurement surfaces, were washed with water and then sterilized with alcohol. The sterilized aluminum plates were then placed in the simulated apparatus and dried for 10 min. After that, the ventilation fan was operated at an airflow rate of 300 m^3/h for 24 h, introducing outdoor air into the simulated apparatus. The microbial contamination on the surface of the aluminum plates was due to fungi from the outdoor air. After 24 h, the ventilation fan was stopped, and the UV lamp installed in the simulated apparatus was activated for the exposure times corresponding to each experimental condition.

Table 4. The experimental conditions for sterilization (levels of exposure doses).

Exposure time	15 min	30 min *	60 min
Dosage (mW·s/cm^2) **	140.4	280.8	561.6

*: Irradiation time required for 99.9% sterilization; **: This is the average value measured multiplied by the time (seconds).

4.3. Measurement Methods

A stamp-type PDA was used to measure the fungal count on the surface of the aluminum plates. Additionally, ATP concentration was also measured. This experiment is the same as described in Section 3.2: see Figure 5 or Figure 6.

4.4. Results and Discussion

Figure 12 shows the changes in fungal count and ATP concentration due to sterilization, and Figure 13 shows photographs of fungal cultures. The average fungal count on the aluminum plate surface before UV lamp sterilization was 127 cfu/25 cm^2. After 15 min of UV lamp exposure, the fungal count ranged from 5 to 9 cfu/25 cm^2, and after 30 min of exposure, the count ranged from 4 to 6 cfu/25 cm^2. Not all fungi were eradicated with sterilization exposure times of 15-to-30 min. The reason for this is that the sterilization exposure dose was calculated based on *Aspergillus niger* (NBRC 6341), and it is possible that some fungi from the outdoor air required a higher exposure dose for sterilization than *Aspergillus niger*. However, with an exposure time of 60 min, which is twice the sterilization exposure dose for *Aspergillus niger*, no fungi were cultured. The results of this measurement indicate that exposing a microbially contaminated surface to UV lamps for 15-to-30 min can achieve a sterilization rate of 94.5%-to-96.1%. Furthermore, doubling the exposure time to 60 min for *Aspergillus niger* (NBRC 6341) resulted in a sterilization rate of 99.9%.

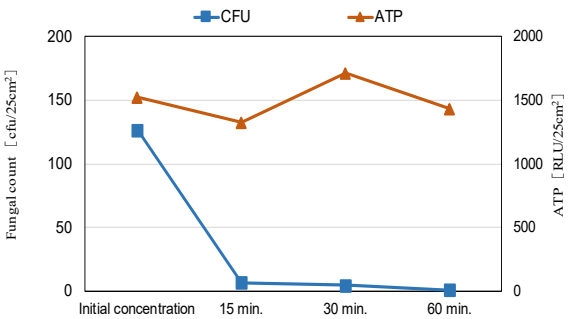

Figure 12. The changes in fungal count and ATP concentration due to sterilization.

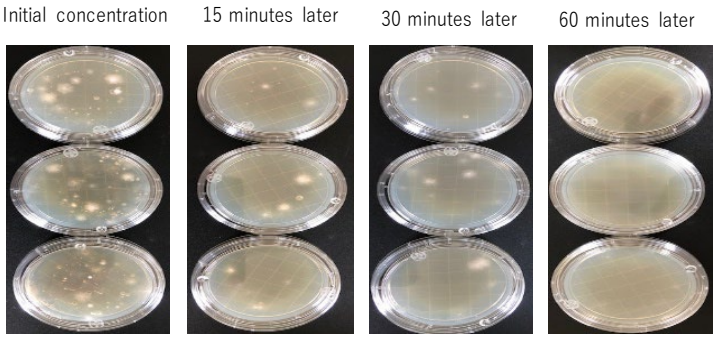

Figure 13. The photographs of fungal cultures.

Generally, UV lamp sterilization in buildings is applied in HVAC systems to sterilize microorganisms or viruses in the air passing through ducts [23]. However, factors such as duct size, air velocity, and the UV lamp's sterilization intensity must be considered [24]. Additionally, the sterilization efficiency of low-pressure mercury UV lamps varies with temperature changes, making it essential to understand and consider these characteristics. Typically, the air temperature in HVAC systems ranges from 5 to 35 °C, with air velocities of 0.5~4 m/s [25,26]. In this study, air temperatures ranged from 25 to 28 °C, and air velocity was approximately 0.5 m/s in a system utilizing geothermal energy in summer. However, this study was not aimed at sterilizing microorganisms in the air, but rather microorganisms attached to the surface of geothermal heat pipes. Consequently, the results of this study cannot be directly compared to those of previous studies; however, the sterilization effect can still be evaluated. Recent studies report extensively on the sterilization efficiency for coronaviruses. The attachment of microorganisms on the cooling coil surface can reduce heat transfer efficiency, increase airflow resistance, and ultimately elevate the energy consumption of the fan and chiller plant. Studies have reported that applying an ultraviolet germicidal irradiation (UVGI) system to the air handling unit (AHU) can clean the coil, enhance coil performance, and contribute to energy savings [27,28]. Additionally, studies show duct air velocities of 1.5~3 m/s, with temperatures between 21 and 25 °C, and UV doses ranging from 2.47 to 423 J/m^2 [29,30]. Under these conditions, reported sterilization efficiencies vary from 39 to 100%, suggesting a strong correlation with both air velocity and UV lamp intensity. When air velocity is high and UV intensity is low, sterilization efficiency tends to decrease. In this study, however, the sterilization effect was measured for microorganisms attached to duct surfaces, and it is believed that the attachment duration of microorganisms on surfaces has a more significant impact on sterilization than air velocity. To enhance system sterilization efficiency, it is recommended to increase exposure time or UV lamp intensity. Moreover, this study suggests the potential presence of microorganisms on HVAC duct surfaces. By sterilizing both airborne microorganisms and those on duct surfaces, cleaner air is expected to be supplied indoors.

5. Conclusions

In this study, a simulated apparatus was constructed to model an air circulation geothermal ventilation system, and the microbial contamination levels on the inner surfaces of the pipes were measured. Additionally, the surface sterilization effect of UV lamps was evaluated.

The fungal concentration on the surface of the aluminum plates within the simulated apparatus showed a tendency to increase over time. However, the adhesion of outdoor-derived contaminants to the surface is influenced not only by airflow (wind speed) but also by the outdoor air temperature, relative humidity, and surface condensation conditions inside the pipes. Therefore, future research should consider these factors as well.

Based on the ATP measurement results, the contamination due to microorganisms was evaluated as "slightly dirty" after 24 h and "dirty" after 48 h of operating the experimental apparatus. Therefore, it is recommended that the internal surfaces of the geothermal

ventilation system be cleaned every 1 to 2 days. Given the observed correlation between fungal counts and ATP measurements, ATP measurement can be considered an effective method for the simple assessment of microbial contamination levels in the field.

The results of the sterilization experiment using UV lamps confirmed that it is possible to inactivate microorganisms derived from outdoor air. The measurements indicated that a microbial-contaminated surface can be sterilized by 94.5%-to-96.1% with 15-to-30 min of UV lamp exposure. However, since the sterilization exposure dose varies depending on the type of microorganism, it is necessary to determine the optimal exposure time based on the type of target fungi and the intensity of the UV lamp exposure.

Funding: This research was supported by Grant-in-Aid for Scientific Research(c) (2020–2022) and the Kurume Institute of Technology President's Discretionary Research Grant (2023).

Data Availability Statement: The original contributions presented in the study are included in the article, further inquiries can be directed to the corresponding author.

Conflicts of Interest: The authors declare no conflict of interest.

References

1. Main Roles of the Cabinet Office, Japan. Available online: https://www8.cao.go.jp/cstp/moonshot/sub4.html (accessed on 20 June 2021).
2. Japan Center for Climate Change Actions. Available online: http://www.jccca.org/chart/chart04_04.html (accessed on 17 April 2018).
3. Ministry of the Environment Website, Japan—Geothermal Energy Utilization Brochure. Available online: http://www.env.go.jp/water/jiban/pamph_gh/index.html (accessed on 11 March 2017).
4. Hasegawa, F. Chapter 7: Unsteady Heat Transfer. In *Principles of Architectural Planning II*; Watanabe, K., Ed.; Maruzen: Tokyo, Japan, 1965.
5. Tarumi, H.; Minohara, Y. Surveillance study on the subterranean thermal use effect of a heat & cool tube residence—About the detached model house which locate in Hokuriku region. *J. Environ. Eng. (Trans. AIJ)* **2010**, *75*, 423–429.
6. Hasegawa, F.; Yoshino, H.; Ishikawa, Y.; Sora, T. Experimental study on cooling performance of the earth tube connected to passive solar test house (Part 2. Terformance of the tube with the lenghth of 45 meters which was embedded in the earth around the test house). *Jpn. Sol. Energy Soc.* **1991**, *17*, 26–36.
7. Sasaki, M.; Ishikawa, Y.; Yoshino, H. *Long-Term Measurement Results of Indoor Thermal Environment and Thermal Performance of Cool Tubes in Naturally Energized Houses Constructed in Sendai City*; Transactions of the Architectural Institute of Japan, Tohoku Branch: Tohoku, Japan, 1995; pp. 145–148.
8. Zhang, Q.; Ishihara, O. Discussion on the exit temperature and cooling energy of cooling tubes for design study on effects of cooling tubes on indoor thermal environment Part 2. *J. Archit. Plan. Environ. Eng.* **1995**, 11–18.
9. Hokoi, S.; Ueda, S.; Yoshida, T. Study on the cooling Effect of cool tube. In *Summaries of Technical Paper of Annual Meeting*; Architectural Institute of Japan: Tokyo, Japan, 1995; pp. 495–496.
10. Azumi, H.; Sakurai, Y. Thermal behavior in a cooking tube system with natural ventilation. *J. Archit. Plan. Environ. Eng.* **2001**, *547*, 33–39.
11. Ueda, S.; Hokoi, S.; Yoshida, T. Cooling Effect of cool tube—In the case of the wet tube surface. In *Summaries of Technical Paper of Annual Meeting*; Architectural Institute of Japan: Tokyo, Japan, 1996; pp. 505–506.
12. Yoon, G.-Y.; Tanaka, H.; Okumiya, M. Exchanged heat charecteristics of the multi-cool/heat tube with close arrangement—Performance perdiction and desing method for the multi-cool/heat tube with close arrangement Part 1. *J. Environ.* **2004**, *579*, 45–52.
13. Ueda, S.; Hokoi, S. Cooling Effect of Cool Tube—In the case of simultaneous heat and moisture transfer in the ground. In *Summaries of Technical Paper of Annual Meeting*; CD recording; Architectural Institute of Japan: Tokyo, Japan, 1997; pp. 411–412.
14. Ishida, M.; Koganei, M.; Kuwahara, R.; Kim, H.; Kohno, H.; Shoda, N.; Yamashita, T. Evaluation of cooling performance and mold removal effectiveness in geothermal ventilation system. In Proceedings of the Annual Research Meeting; Chugoku Chapter; CD recording. Architectural Institute of Japan: Tokyo, Japan, 2018; pp. 421–424.
15. Kishida, S.; Yoshihara, M.; Kim, H.; Koganei, M.; Hashimoto, M.; Hatano, M.; Hasegawa, M.; Ueda, K.; Hamai, R. Study on Particulate Removal Efficiency in the Geothermal Ventilation System. In Proceedings of the Annual Research Meeting; Chugoku Chapter. Architectural Institute of Japan: Tokyo, Japan, 2021; pp. 365–368.
16. *AIJES-A0008*; Standards and Commentary for Sampling Methods of Airborne Microorganisms. Architectural Institute of Japan: Tokyo, Japan, 2013.
17. Adenosine Triphosphate Measurement Method. Available online: https://ja.wikipedia.org/wiki/ATP (accessed on 22 July 2020).
18. NITTA Corporation (ATP Swab Test Kit) Luminometer (Japanese User Manual), SystemSURE Operation Manual V3.0 (2013). Available online: https://nitta-monitoring.com/sanitary/food/atp-ruminometer/ (accessed on 22 July 2020).

19. Matsumura, M.; Fujiwara, M.; Ogata, M.; Tsutsumi, H.; Hori, S.; Tanabe, S.-i. Environmental surface contamination measured by ATP assay and attitube surve of medical and cleaning staff in the examination room. *J. Environ. Eng.* **2016**, *81*, 893–899. [CrossRef]
20. Ogata, M.; Iigima, M.; Matsumura, M.; Tsutsumi, H.; Hori, S.; Tanabe, S.-i. Environmental surface contamination examined by ATP assay before and after terminal room cleaning in patient rooms. *J. Environ. Eng.* **2016**, *81*, 723–729. [CrossRef]
21. Yanagi, U. Microbiol contamination in an air-conditioning system and countermeasure against mould smell. *J. Jpn. Assoc. Odor Environ.* **2012**, *43*, 191–198.
22. Sung, M.; Kato, S.; Yanagi, U. Evaluation of surface and air disinfection effects using UV radition simulation. *J. Environ. Eng.* **2009**, *74*, 1137–1143. [CrossRef]
23. Capetillo, A.J. Computational Fluid Dynamic Modeling of In-Duct UV Air Sterilisation Systems. 2015. Available online: http://etheses.whiterose.ac.uk/9591/ (accessed on 25 October 2024).
24. Philips, U.V. Purification—Application Information. Volume 39. 2005. Available online: https://www.assets.signify.com/is/content/Signify/Assets/philips-lighting/global/20230816-uv-c-disinfection-application-guide-dec21.pdf (accessed on 25 October 2024).
25. Lau, J.; Bahnfleth, W.; Freihaut, J. Estimating the effects of ambient conditions on the performance of UVGI air cleaners. *Build. Environ.* **2009**, *44*, 1362–1370. [CrossRef]
26. Zhang, H.; Jin, X.; Nunayon, S.S.; Lai, A.C.K. Disinfection by in-duct ultraviolet lamps under different environmental conditions in turbulent airflows. *Indoor Air* **2020**, *30*, 500–511. [CrossRef] [PubMed]
27. Wang, Y.; Sekhar, C.; Bahnfleth, W.P.; Cheong, K.W.; Firrantello, J. Effectiveness of an ultraviolet germicidal irradiation system in enhancing cooling coil energy performance in a hot and humid climate. *Energy Build.* **2016**, *130*, 321–329. [CrossRef]
28. Luongo, J.C.; Miller, S.L. Ultraviolet germicidal coil cleaning: Decreased surface microbial loading and resuspension of cell clusters. *Build. Environ.* **2016**, *105*, 50–55. [CrossRef]
29. Yang, Y.; Zhang, H.; Nunayon, S.S.; Chan, V.; Lai, A.C.K. Disinfection efficacy of ultraviolet germicidal irradiation on airborne bacteria in ventilation ducts. *Indoor Air* **2018**, *28*, 806–817. [CrossRef] [PubMed]
30. Luo, H.; Zhong, L. Ultraviolet germicidal irradiation (UVGI) for in-duct airborne bioaerosol disinfection: Review and analysis of design factors. *Build. Environ.* **2021**, *197*, 107852. [CrossRef] [PubMed]